The Chalcone Flavokawain B Induces G$_2$/M Cell-Cycle Arrest and Apoptosis in Human Oral Carcinoma HSC-3 Cells through the Intracellular ROS Generation and Downregulation of the Akt/p38 MAPK Signaling Pathway

You-Cheng Hseu,[†] Meng-Shiou Lee,[‡] Chi-Rei Wu,[‡] Hsin-Ju Cho,[§] Kai-Yuan Lin,[∥] Guan-Hua Lai,[⊥] Sheng-Yang Wang,[#] Yueh-Hsiung Kuo,[‡] K. J. Senthil Kumar,*,[†] and Hsin-Ling Yang*,[§]

[†]Department of Cosmeceutics and [‡]School of Chinese Pharmaceutical Sciences and Chinese Medicine Resources, College of Pharmacy, China Medical University, Taichung 40402, Taiwan

[∥]Department of Medical Research, Chi-Mei Medical Center, Tainan 71004, Taiwan

[⊥]Graduate Institute of Biotechnology, College of Agriculture and Natural Resources, and [#]Department of Forestry, National Chung Hsing University, Taichung 40402, Taiwan

[§]Institute of Nutrition, China Medical University, Taichung 40402, Taiwan

ABSTRACT: Chalcones have been described to represent cancer chemopreventive food components that are rich in fruits and vegetables. In this study, we examined the anti-oral cancer effect of flavokawain B (FKB), a naturally occurring chalcone isolated from *Alpinia pricei* (shell gingers), and revealed its molecular mechanism of action. Treatment of human oral carcinoma (HSC-3) cells with FKB (1.25−10 μg/mL; 4.4−35.2 μM) inhibited cell viability and caused G$_2$/M arrest through reductions in cyclin A/B1, Cdc2, and Cdc25C levels. Moreover, FKB treatment resulted in the induction of apoptosis, which was associated with DNA fragmentation, mitochondria dysfunction, cytochrome *c* and AIF release, caspase-3 and caspase-9 activation, and Bcl-2/Bax dysregulation. Furthermore, increased Fas activity and procaspase-8, procaspase-4, and procaspase-12 cleavages were accompanied by death receptor and ER-stress, indicating the involvement of mitochondria, death-receptor, and ER-stress signaling pathways. FKB induces apoptosis through ROS generation as evidenced by the upregulation of oxidative-stress markers HO-1/Nrf2. This mechanism was further confirmed by the finding that the antioxidant *N*-acetylcysteine (NAC) significantly blocked ROS generation and consequently inhibited FKB-induced apoptosis. Moreover, FKB downregulated the phosphorylation of Akt and p38 MAPK, while their inhibitors LY294002 and SB203580, respectively, induced G$_2$/M arrest and apoptosis. The profound reduction in cell number was observed in combination treatment with FKB and Akt/p38 MAPK inhibitors, indicating that the disruption of Akt and p38 MAPK cascades plays a functional role in FKB-induced G$_2$/M arrest and apoptosis in HSC-3 cells.

KEYWORDS: *flavokawain B, cell-cycle arrest, apoptosis, ROS, Akt, p38 MAPK, HSC-3 cells*

■ INTRODUCTION

Oral cancer is one of the 10 most frequently occurring cancers worldwide, and its prevalence in Europe and the United States ranges from 2 to 6% among all cancer patients.[1] A wide variation exists in the incidence and mortality rates of oral cancer in different regions around the world. The highest rates have been reported in South Asia and Asia Pacific regions, especially India, Sri Lanka, Taiwan, Japan, and Australia, and the incidence and mortality in these regions are almost twice those of the global rates.[2] The treatment of oral cancer has primarily relied on classical modalities encompassing surgery, radiation, and chemotherapy or a combination of these methods.[1] Thus, the development of effective chemopreventive or chemotherapeutic agents/approaches using nontoxic botanicals may represent one strategy for the management of oral cancers.

Chemoprevention, which refers to the administration of natural or chemically synthesized agents to prevent initiating and promotional events associated with carcinogenesis, is increasingly being considered an effective approach for the management of neoplasms.[3] Treatment with chemopreventive or chemotherapeutic agents that regulate cell-cycle machinery result in cell-cycle arrest in different phases. Therefore, controlling the growth and proliferation of cancerous cells and inducing apoptosis are major goals of cancer chemoprevention.[4] Eukaryotic cell-cycle progression involves the sequential activation of cyclin-dependent kinases (CDKs), which is dependent upon association with cyclins. Progression through the mammalian mitotic cycle is controlled by multiple holoenzymes, including a catalytic CDK and a cyclin regulatory subunit.[5] These cyclin−CDK complexes are activated at synchronized intervals during the cell cycle. However, CDKs can be induced and regulated by exogenous factors, such as UV light, ionizing radiation, thermal disruption and industrial chemicals.[3,4] Apoptosis is a complex process of deliberate suicide by a cell in a multicellular organism. Apoptosis represents one of the main types of programmed cell death and involves an orchestrated series of biochemical events leading to a characteristic cell morphology and death; features of apoptosis

include cellular morphological changes, chromatin condensation, internucleosomal DNA cleavage, and the activation of a family of cysteine-aspartic acid proteases (caspases).[6] Chemical and biological agents that induce cell-cycle arrest and apoptosis have been reported to be promising interventions in the management of malignant cancer.

The rhizomes of *Alpinia* plants (family Zingiberaceae, which includes ginger, turmeric, and cardamon plants) are widely used as culinary spices in Asian countries, eaten raw, cooked as vegetables, or used as food flavoring. *Alpinia pricei* Hayata (shell gingers) is a perennial rhizomatous plant indigenous to Taiwan. This plant has various traditional and commercial applications, such as the use of the leaves to make traditional zongzi (glutinous rice dumplings) and the use of the aromatic rhizomes as a folk medicine for dispelling abdominal distension and enhancing stomach secretion and peristalsis.[7] Recent studies have reported that *Alpinia* plants possess a variety of biological activities, including antioxidant,[8,9] anti-inflammatory,[7,10] anticancer,[11,12] immunostimulating,[13] hepatoprotective,[14] and antinociceptive[10] activities. Our previous studies have demonstrated that ethanol extracts of *Alpinia pricei* exhibit antitumor effects by inducing cell-cycle arrest and apoptosis in human squamous carcinoma KB cells.[11,12] However, the phytochemistry and bioactivity of *Alpinia pricei* extracts have not yet been elucidated.

Chalcones (1,3-diaryl-2-propen-1-ones) are precursors in the biosynthesis of flavonoids/isoflavonoids and are cancer preventive food components in a human diet that is rich in fruits and vegetables. Detailed investigations have revealed that flavokawain B (FKB), a chalcone derivative in kava extracts used by South Pacific Islanders for thousands of years, has strong antiproliferative effects against several cancer cell lines.[11,15−17] An epidemiologic study has found that the cancer incidence in the three highest kava-drinking countries (Vanuatu, Fiji, and Western Samoa) is one-fourth to one-third of that in non-kava-drinking countries, such as New Zealand (Maoris) and the United States (Hawaii and Los Angeles).[17−19] These findings should encourage the development of more potent chalcone derivatives for both the prevention and treatment of cancer, as well as epidemiologic studies of the relationship between kava consumption and cancer. The chemopreventive properties of flavokawain B combined with the epidemiologic and experimental data prompted this study of the inhibitory effects of treatment with flavokawain B on human oral cancer cells. Therefore, in an effort to develop an effective chemotherapeutic agent for the prevention of oral cancers, we examined the chemotherapeutic effect of FKB purified from 70% ethanol extracts of *Alpinia pricei* rhizomes on human oral cancer HSC-3 cells. We show that FKB (1.25−10 μg/mL) inhibits growth and proliferation and induces apoptosis in HSC-3 cells. Our study also provides insight into the mechanism by which FKB induces cell-cycle arrest and apoptosis in HSC-3 cells.

■ MATERIALS AND METHODS

Reagents. Dulbecco's modified Eagle medium (DMEM), Roswell Park Memorial Institute (RPMI-1640) medium, nutrient mixture F-12, fetal bovine serum (FBS), glutamine, and penicillin/streptomycin were purchased from Invitrogen/Gibco BRL (Grand Island, NY). Antibodies against cyclin B1, Cdc2, cytochrome *c*, Bcl-2, Bax, Fas, FasL, Nrf2, and ERK1/2 were obtained from Santa Cruz Biotechnology Inc. (Heidelberg, Germany). The rabbit polyclonal anti-PARP antibody was purchased from Roche (Mannheim, Germany). The antibody against *β*-actin and the MTT (3-[4,5-dimethyl-2-yl]-2,5-diphenyltetrazolium bromide) were purchased from Sigma-Aldrich (St. Louis, MO).

Antibodies against cyclin A, Cdc25C, caspase-3, caspase-9, p-Akt, Akt, PI3K, JNK1/2, and p38 were obtained from Cell Signaling Technology Inc. (Danvers, MA). The antibody against caspase-4 was obtained from BIOMOL Inc. (Montgomery, PA), The antibody against caspase-12 was purchased from Millipore Inc. (Temecula, CA), and the antibodies against caspase-8 were obtained from NeoMarkers Inc. (Fremont, CA). Anti-rabbit polyclonal HO-1, p-JNK1/2, p-ERK1/2, and p-p38 were purchased from Abcam (Cambridge, U.K.), and the antibody against HSP70 was purchased from BD Transduction Laboratories (Hayward, CA). DAPI (4′,6-diamidino-2-phenylindole dihydrochloride), the Akt inhibitor LY294002, the p38 inhibitor SB203580, the ERK inhibitor PD98059, and the JNK inhibitor SP600125 were obtained from Calbiochem (La Jolla, CA). All other chemicals were reagent grade or HPLC grade and supplied by either Merck & Co. Inc. (Darmstadt, Germany) or Sigma-Aldrich (St. Louis, MO).

Isolation and Characterization of FKB. Air-dried rhizomes (2 kg) from *Alpinia pricei* were extracted with 10 L of 70% (v/v) ethanol at room temperature as previously described.[11,19,20] We further characterized the main composition of the *A. pricei* extracts using chromatography followed by spectral analysis. The *A. pricei* extracts were separated by semipreparative HPLC. A Luna silica column (250 mm × 10 mm, Phenomenex Co., Torrance, CA) was employed with two solvent systems: A, H_2O; B, acetonitrile. The gradient elution profile was as follows: 0−3 min, 80% (v/v) A to B; 3−60 min, 80−0% A to B (linear gradient); 60−80 min 0% A to B; the flow rate was 2.5 mL/min and the detector wavelength was set at 280 nm. The three major compounds in the *A. pricei* extracts were obtained at retention times of 32.5 min (**1**), 37.0 min (**2**) and 46.7 min (**3**). The structures of compounds **1−3** were determined by spectroscopic analysis. The UV spectra of these compounds were recorded with a Jasco V-550 spectrometer, and the IR spectra were obtained with a Bio-Rad FTS-40 spectrophotometer. Electron-impact mass spectrometry (EIMS) and high-resolution electron-impact mass spectrometry (HREIMS) data were collected with a Finnigan MAT-958 mass spectrometer. The NMR spectra were recorded with Bruker Avance 500 and 300 MHz FT-NMR spectrometers at 500 MHz (^{1}H) and 75 MHz (^{13}C). According to the mass and NMR analysis, compounds **1−3** were identified as follows: **1**, desmethoxyyangonin; **2**, cardamonin; and **3**, flavokawain B (FKB).[19] The standard calibration curves (peak area vs concentrations) of compounds **1−3** ranged from 5 to 100 μg/mL. According to the results of HPLC analysis, the amounts of the compounds desmethoxyyangonin, cardamonin, and FKB in the *A. pricei* extracts were 1.1%, 8.9%, and 5.7%, respectively. The obtained FKB (Figure 1A) purity was above 99%, which was confirmed by HPLC and ^{1}H NMR analysis. A stock solution of FKB (10 mg/mL or 35.2 mM) was prepared in 100% DMSO and subsequently diluted in medium so that the final concentration of DMSO was 0.1% in the medium.

Cell Cultures and Sample Treatments. Human oral squamous carcinoma (HSC-3), human melanoma (A-2058), oral adenosquamous carcinoma (Cal-27), and lung carcinoma (A-549) cells were obtained from the American Type Culture Collection (ATCC, Rockville, MD). HSC-3 cells were grown in DMEM/F-12 (1:1) supplemented with 10% (v/v) heat-inactivated FBS, 1.5 g/L sodium bicarbonate, and 1% penicillin/streptomycin. The A2058 cells were grown in DMEM supplemented with 10% FBS, 2 mM glutamine, 3.7 g/L sodium bicarbonate, 2% nonessential amino acids, and 1% penicillin/streptomycin. The Cal-27 cells were grown in DMEM supplemented with 10% FBS, 2 mM glutamine, 3.7 g/L sodium bicarbonate, and 1% penicillin/streptomycin. The A-549 cells were grown in RPMI-1640 supplemented with 10% FBS, 2 mM glutamine, 2 g/L sodium bicarbonate, and 1% penicillin/streptomycin. The cells were maintained in an incubator with a humidified atmosphere of 95% air and 5% CO_2 at 37 °C. The final concentration of DMSO in all experiments was adjusted to 0.1% (v/v). In additional experiments, HSC-3 cells were pretreated with 2.5 mM NAC and 10−30 μM Akt (LY294002), 10−30 μM p38 (SB203580), 25−50 μM ERK (PD98059), or 15−30 μM JNK (SP600125) inhibitors for 1 h followed by incubation with or without the indicated concentration of FKB for 24 h.
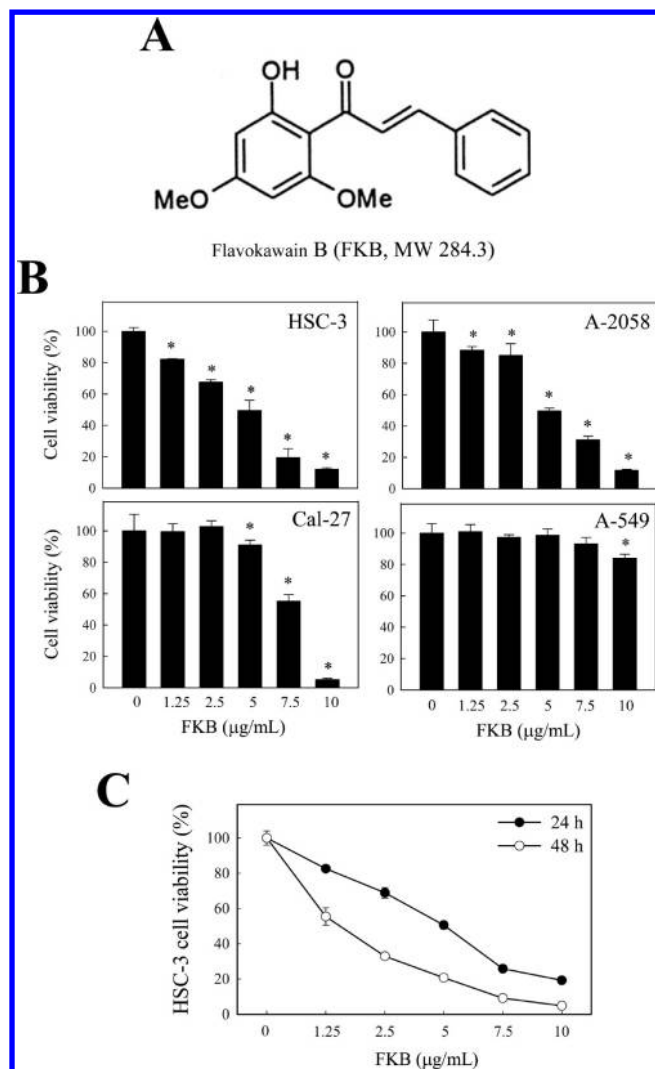
Figure 1. FKB inhibits the growth of human cancer cells. (A) Chemical structure of FKB. (B) HSC-3, A2058, Cal-27, and A549 cells (5×10^4 cells/well) were treated with different concentrations of FKB (1.25–10 μg/mL) and grown in 24-well plates for 24 h. Vehicle alone (0.1% DMSO in media) served as the control. (C) HSC-3 cells were treated with FKB (1.25–10 μg/mL) for 24 and 48 h. The inhibitory effects of FKB were determined by MTT assay. Cell viability (%) was calculated as $[(A_{570}$ of treated cells)/$(A_{570}$ of untreated cells)$] \times 100$. Each value is expressed as the mean $\pm$ SD ($n = 3$). *Significant difference compared with the control group ($p < 0.05$).

Cell Viability Assay. The effect of FKB on cell viability was monitored by the MTT colorimetric assay, as previously described.[15] In brief, after overnight incubation, cells were treated with various concentrations of FKB (0, 1.25, 2.5, 5, 7.5, and 10 μg/mL [0, 4.4, 8.8, 17.6, 26.4, and 35.2 μM]) for 24 or 48 h. The culture supernatants were removed, and 500 μL of MTT (0.5 mg/mL) in PBS was added into each well. After incubation at 37 °C for 2 h, 300 μL of isopropanol was added to dissolve the MTT formazan crystals. The absorbance was then measured at 570 nm, and the obtained values were compared with the MTT standard cure. The effect of FKB on cell viability was assessed as the percent of viable cells compared with the vehicle-treated control, which was arbitrarily assigned 100% viability. The assay was performed in triplicate for each concentration.

Cell-Cycle Analysis. Cellular DNA content was determined by flow cytometric analysis with propidium iodide (PI)-labeled cells as previously described.[15] HSC-3 cells were seeded at a density of 4×10^5 cells/10 cm dish for overnight incubation, and the synchronization of the cell cycle was achieved using a double thymidine block. Briefly,

HSC-3 cells were treated with 3 mM thymidine in DMEM medium containing 10% FBS for 16 h. After treatment, the cells were washed twice with PBS and then cultured in fresh medium for another 10 h. The cells were then blocked with DMEM medium containing 3 mM thymidine for 16 h. Cell-cycle synchronized cells were then washed with PBS and restimulated to enter the G_1 phase together by addition of fresh DMEM medium containing FKB (1.25–10 μg/mL). The cells were harvested at 24 h by trypsinization and then fixed in 3 mL of ice cold 70% ethanol at −20 °C overnight. Cell pellets were collected by centrifugation, resuspended in 500 μL of PI staining buffer (1% Triton X-100, 0.5 mg/mL RNase A, and 4 μg/mL PI in PBS), and incubated at room temperature for 30 min. The cell-cycle progression was detected on a FACScan cytometer (BD Biosciences, San Jose, CA) equipped with a single argon ion laser (488 nm). The forward and right-angle light-scattering, which correlates with cell size and cyto-plasmic complexity, respectively, were used to establish size gates and exclude cellular debris from the analysis. The DNA content of 1×10^4 cells/analysis was monitored using the BD FACSCalibur system. The cell-cycle profiles were analyzed with ModFit software (Verity Software House, Topsham, ME).

Determination of Apoptosis. Apoptotic cell death was measured using terminal deoxynucleotidyl transferase-meditated dUTP-fluores-cein nick end-labeling (TUNEL) with the fragmented DNA detection kit (Roche, Mannheim, Germany) following the supplier's instruction. Cells (2×10^4 cells/well) were seeded on eight-well Tek chambers (Nunc, Denmark) and treated with various concentrations of FKB (0, 1.25, 2.5, 5, 7.5, and 10 μg/mL) for 24 h. After incubation, the cells were washed with PBS twice, fixed in 2% paraformaldehyde for 30 min, and permeabilized with 0.1% Triton X-100 for 30 min at room temperature. The cells were then incubated with TUNEL reaction buffer in a 37 °C humidified chamber for 1 h in the dark, rinsed twice with PBS, and incubated with DAPI (1 mg/mL) at 37 °C for 5 min; images of the stained cells were obtained under a fluorescence micro-scope.

Fluorescent Imaging of Mitochondrial and Endoplasmic Reticulum (ER) Activity. Fluorescent imaging of mitochondria and endoplasmic reticulum was accomplished using a Mito-Tracker Green or ER-Tracker Green detection kit (Molecular Probe, Eugene, OR) following the manufacturer's instructions. Mito-Tracker is a green fluorescent mitochondrial stain that appears to localize to mitochon-dria regardless of mitochondrial membrane potential. ER-Tracker green dye is a cell-permeant, live-cell stain that is highly selective for the ER. HSC-3 cells (2×10^4 cells/well) were seeded on eight-well Tek chambers and treated with various concentrations of FKB (0, 1.25, 2.5, 5, 7.5, and 10 μg/mL) for 24 h. After FKB treatment, the cells were fixed in 2% paraformaldehyde in PBS for 15 min and then incubated with 1 μM Mito-Tracker for 30 min or 2 μM ER-Tracker for 60 min. The cells were stained with 1 μg/mL DAPI for 5 min, and stained cells were visualized using a fluorescence microscope at 400× magnification.

Immunofluorescence Assay. HSC-3 cells (2×10^4 cells/well) were cultured in DMEM/F-12 medium with 10% FBS on glass eight-well Tek chambers. After FKB treatment, the cells were fixed in 2% paraformaldehyde for 15 min, permeabilized with 0.1% Triton X-100 for 10 min, washed/blocked with 10% FBS in PBS, and then incubated for 1 h with anti-HO-1 primary antibody in 1.5% FBS. The cells were incubated with a FITC (488 nm)-conjugated secondary antibody for another 1 h in 6% bovine serum albumin. The cells were stained with 1 μg/mL DAPI for 5 min. Stained cells were washed with PBS and visualized using a fluorescence microscope at 400× magnification.

Measurement of ROS Generation. Intracellular ROS accumu-lation was detected by fluorescence microscopy using the cell-permeable fluorogenic probe 2′,7′-dihydrofluorescein diacetate (DCFH-DA). HSC-3 cells (1×10^5 cells/well; 12-well plate) were cultured in DMEM/F-12 medium supplemented with 10% FBS, and the culture medium was replaced when the cells reached 80% confluence. To evaluate the generation of ROS in a time-dependent manner, cells were treated with 7.5 μg/mL of FKB for 0, 1, 5, 10, 30, and 60 min. After FKB treatment for the indicated time periods, culture super-natants were removed, and the cells were then incubated with 10 μM

DCFH-DA in fresh medium at 37 °C for 30 min. During loading, the acetate groups on DCFH-DA were removed by intracellular esterase, trapping the probe inside the HSC-3 cells. After incubation, the culture medium was removed, and the cells were then washed with warm PBS buffer. The production of ROS can be measured by changes in fluorescence due to the intracellular accumulation of dichlorofluorescein (DCF) caused by oxidation of DCFH. Intracellular ROS, as indicated by DCF fluorescence, was measured with a fluorescence microscope (Olympus 1×71 at 200× magnification).

Western Blot Analysis. HSC-3 cells (7.5×10^5 cells/dish; 10 cm dish) were incubated with or without various concentrations of FKB for 24 h. After incubation, adherent and detached cells were harvested, pooled, washed once in PBS, and then suspended in 100 μL of lysis buffer (10 mM Tris-HCl, pH 8, 320 mM sucrose, 1% Triton X-100, 5 mM EDTA, 2 mM DTT, and 1 mM PMSF). Cell suspensions were kept on ice for 20 min and then centrifuged at $15000g$ for 30 min at 4 °C. Total protein content was determined using Bio-Rad protein assay reagent (Bio-Rad, Hercules, CA) and BSA as a standard. The protein extracts were reconstituted in sample buffer (62 mM Tris-HCl, 2% SDS, 10% glycerol, and 5% β-mercaptoethanol), and the mixture was boiled at 97 °C for 5 min. Equal amounts (50 μg) of denatured protein samples were loaded into each lane, separated by SDS−PAGE on 8−15% polyacrylamide gradient, and then transferred onto a polyvinylidene difluoride (PVDF) membrane overnight. Membranes were blocked with 5% nonfat dried milk in PBS containing 1% Tween-20 for 1 h at room temperature followed by incubation with primary antibodies overnight and either horseradish peroxidase-conjugated goat anti-rabbit or anti-mouse antibodies for 2 h. The blots were detected by ImageQuant LAS 4000 mini (Fujifilm) with the Super-Signal West Pico chemiluminescence substrate (Thermo Scientific, IL). Western blot analyses were performed using antibodies against cytochrome c, AIF, caspase-3, caspase-4, caspase-8, caspase-9 and caspase-12, PARP, Bcl-2, Bax, Fas, FasL, cyclin A, cyclin B1, Cdc2, Cdc25C, HO-1, Nrf2, PI3K, p-Akt, Akt, p-p38, p38, p-JNK1/2, JNK1/2, p-ERK1/2, and ERK1/2. Densitometry analyses were performed using commercially available quantitative software (AlphaEase, Genetic Technology Inc. Miami, FL) with the control representing 1-fold as shown just below the data.

Statistics. In vitro results are presented as the mean ± standard deviation (mean ± SD). All study data were analyzed using an analysis of variance, followed by Dunnett's test for pairwise comparison. Statistical significance was defined as $p < 0.05$ for all tests. Each sample was tested in triplicate.

■ RESULTS

FKB Inhibits the Growth of Human Cancer Cells. Human carcinoma cell lines (HSC-3, A-2058, Cal-27, and A-549) were treated with various concentrations of FKB for 24 h. MTT assay shows that FKB treatment significantly ($p < 0.05$) reduced HSC-3, A-2058, and Cal-27 cell survival in a dose-dependent manner with IC_{50} values of 4.9, 5.2, and 7.6 μg/mL, respectively, indicating the susceptibility of cancer cells to FKB treatment (Figure 1B), whereas FKB exerted a very minimal effect against A-549 cells (Figure 1B). However, the significant cytotoxic effect of FKB (>20 μ/mL) was not observed in normal human gingival fibroblast HGF cells as demonstrated in our previous report.[19] In addition, cell survival was evaluated in a time-dependent fashion. FKB (1.25−10 μg/mL) treatment for 24 and 48 h significantly induced a time- and dose-dependent diminution of HSC-3 cell viability, indicating its potential ability to impair tumor growth (Figure 1C). All treated cells showed a reduction in cell viability, which differed according to the cell type and concentration of drug. However, the reduction was more pronounced in HSC-3 cells than in A-2058, Cal-27, and A-549 cells. These data suggest that FKB has a broad inhibitory effect on the growth and survival of HSC-3 cancer cells.

FKB Treatment Caused G_2/M Cell-Cycle Arrest in HSC-3 Cells. To examine whether FKB treatment could affect the cell-cycle progression of HSC-3 cells, synchronized cells were treated with FKB (5 μg/mL; IC_{50}) for 12, 24, 36, and 48 h and subjected to flow cytometric analysis of DNA staining. Figure 2A
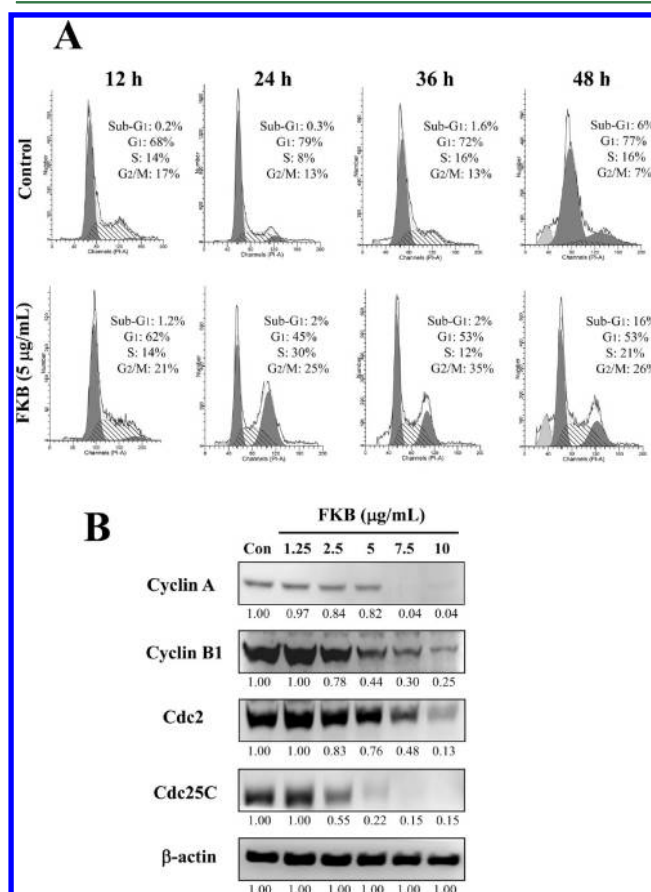
Figure 2. FKB induces G_2/M arrest in human oral carcinoma HSC-3 cells. (A) Cells were treated with or without 5 μg/mL of FKB for 12, 24, 36, and 48 h, stained with PI and analyzed for cell-cycle phase by flow cytometry. Representative flow cytometry profiles are shown. The cellular distributions (percentage) in different phases of the cell cycle (sub-G_1, G_1, S, and G_2/M) were determined after treatment with FKB. (B) The effects of FKB (1.25−10 μg/mL for 24 h) on cell-cycle regulatory protein levels (cyclin A, cyclin B1, Cdc2, and Cdc25C) were examined by Western blot analysis. Protein (50 μg) from each sample was resolved by 8−15% SDS−PAGE with β-actin as a loading control. The photomicrographs shown here are from one representative experiment repeated three times with similar results.

shows that FKB exposure resulted in progressive and sustained accumulation of cells in G_2/M phase. At 12 h after the beginning of the FKB treatment, 21% of the cell population was observed to be in the G_2/M transition phase of the cell cycle, and this percentage reached 25%, 35%, and 26% after 24, 36, and 48 h, respectively. These percentages were comparatively higher than the proportion of cells that were in G_2/M phase (17%, 13%, 13%, and 7% at 12, 24, 36, and 48 h, respectively) in the vehicle (0.1% DMSO) treated cells (Figure 2A). Furthermore, the accumulation of cells in G_2/M phase was accompanied by a decrease in the population of cells in G_1 phase. Indeed, in response to FKB treatment, 62% of the cells were detected in G_1 phase at 12 h, which increased to 45%, 53%, and 53% at 24, 36, and 48 h, respectively, compared with 68%, 79%,

72% and 77% in cells treated with vehicle (0.1% DMSO). Also, flow cytometric analysis showed that a significant sub-G_1 cell population appeared following treatment with FKB for 48 h (Figure 2A). In untreated HSC-3 cells, 6% of cells were PI-positive, whereas 16% of cells were PI-positive after treatment with 5 μg/mL of FKB for 48 h. The percentages of sub-G_1 population at 48 h which are shown in Figure 2A demonstrate the significant increase in the apoptosis at later stage. Moreover, compare to control the percentage of apoptotic cells at 48 h was more than 16%. Therefore, our findings suggest that FKB promotes cell growth inhibition by inducing G_2/M phase arrest and induces apoptosis in HSC-3 oral cancer cells.

FKB Treatment Downregulates Cyclin A, Cyclin B1, Cdc2, and Cdc25C Expression in HSC-3 Cells. Eukaryotic cell-cycle progression involves sequential activation of CDKs, whose activity is dependent upon the formation of complexes with regulatory cyclins.[21] The formation of a complex between Cdc2 (CDK-1) and cyclin A/B1 is an important event for cells to enter into mitosis.[22] Therefore, we hypothesized that the FKB-induced G_2/M cell-cycle arrest may be due to the inhibition of cyclin A, cyclin B1, Cdc2, and Cdc25C, which are critically involved in G_2/M progression. As expected, FKB (1.25−10 μg/mL) treatment for 24 h caused a significant reduction in the protein levels of cyclin A, cyclin B, Cdc2 (mitotic-cyclin dependent kinase), and Cdc25C (mitotic phosphatase) in a dose-dependent manner (Figure 2B). These data imply that FKB inhibits cell-cycle progression by reducing the levels of cyclin A, cyclin B1, Cdc2, and Cdc25C in HSC-3 cells.

FKB Induces Apoptotic DNA Fragmentation in HSC-3 Cells. To further define the mechanism of cell death caused by FKB, HSC-3 cells were treated with FKB (1.25−10 μg/mL) for 24 h, and DNA fragmentation was measured by the TUNEL assay. FKB treatment for 24 h caused active apoptosis, and DNA single-strand breaks were labeled with dUTP-fluorescein at the 3′-OH ends of nuclei (Figure 3A). In the control cells and those treated with a lower concentration of FKB (1.25 μg/mL) for 24 h, the green fluorescence intensity was almost undetectable. However, increases in the fluorescence intensity were observed in a dose-dependent manner (Figure 3A). These data demonstrate that FKB treatment effectively induces apoptosis in HSC-3 cells.

FKB Treatment Induces Mitochondrial Membrane Permeability in HSC-3 Cells. We further examined whether the FKB-induced apoptosis was mediated by the mitochondrial pathway. HSC-3 cells were treated with FKB (1.25−10 μg/mL) for 24 h, and changes in the mitochondrial membrane potential were monitored using a Mito-Tracker assay kit as described in Materials and Methods. Mito-Tracker is a green fluorescent dye that stains mitochondria in live cells, and its accumulation is dependent upon membrane potential. Bright green fluorescence was observed in the control cells, whereas exposure of cells to FKB for 24 h caused a dose-dependent decrease in the green fluorescence, indicating that FKB treatment induced mitochondrial membrane permeability in HSC-3 cells (Figure 3A). These data are direct evidence that mitochondrial function is critically impaired in FKB-induced apoptosis in HSC-3 cells.

FKB Treatment Upregulates the Mitochondrial Apoptotic Cascades in HSC-3 Cells. A number of key protein markers involved in mitochondria-mediated apoptosis were also examined by Western blot analysis. Initially, we determined the levels of cytochrome c in both mitochondrial and cytosolic fractions. The incubation of cells with FKB resulted in a reduction
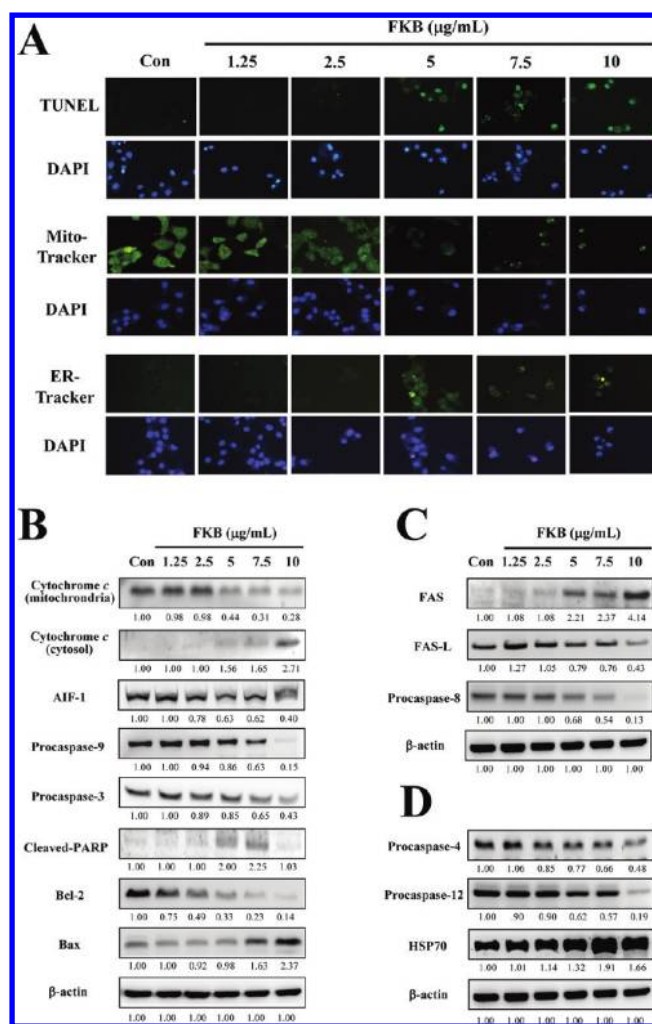
Figure 3. FKB-induced apoptosis in HSC-3 cells. (A) TUNEL assay was performed to determine apoptotic DNA fragmentation. HSC-3 cells were exposed to FKB (1.25−10 μg/mL, 24 h). The green florescence indicates the average number of apoptotic-positive cells in microscopic fields (magnification ×400) from three separate samples (upper panel). The effects of FKB (1.25−10 μg/mL for 24 h) on the mitochondrial activity and endoplasmic reticulum distribution in HSC-3 cells. The activity of the mitochondria was determined by uptake of Mito-Tracker (green CMXRos) of mitochondria (middle panel). Fluorescent imaging of endoplasmic reticulum was accomplished using ER-Tracker (Green glibenclamide-BODIPY FL) (lower panel). After FKB treatment, HSC-3 cells were incubated for 60 min with 2 μM ER-Tracker or for 30 min with 1 μM Mito-Tracker at 37 °C. The cells were incubated with DAPI (1 μg/mL) for 5 min and examined by fluorescence microscopy (magnification ×300) as described in Materials and Methods. (B−D) Western blot analysis of apoptotic-related proteins in HSC-3 cells exposed to FKB. (B) The effects of FKB (1.25−10 μg/mL, 24 h) on the protein levels of mitochondrial and cytosolic cytochrome c, AIF, caspase-9, caspase-3, PARP, Bcl-2, and Bax (mitochondrial pathway); (C) Fas, FasL, and caspase-8 (death receptor pathway); (D) caspase-4, caspase-12, and HSP70 (ER stress pathway) in HSC-3 cells. Protein (50 μg) from each sample was resolved by 8−15% SDS−PAGE with β-actin as a control. The photomicrographs shown here are from one representative experiment repeated twice with similar results.

in cytochrome c in mitochondria. Conversely, increased cytochrome c levels were detected in the cytosolic fraction (Figure 3B). The FKB-induced release of cytochrome c from the mitochondria into the cytoplasm occurred in a concentration-dependent fashion and reached a plateau at 10 μg/mL.

Cytochrome *c* is reportedly involved in the activation of the downstream caspases that trigger apoptosis.[11] We investigated the roles of caspase-9 and caspase-3 in the cellular response to FKB. Western blot analysis showed that treatment of HSC-3 cells with FKB induced the proteolytic cleavage of procaspase-9 (47 kDa) and procaspase-3 (35 kDa) into their active forms (Figure 3B). PARP-specific proteolytic cleavage by caspase-3 is considered to be a biochemical characteristic of apoptosis. Figure 3B also shows that, in response to FKB treatment, the 115 kDa PARP protein is cleaved into a 85 kDa fragment in HSC-3 cells. The Bcl-2 family proteins are critical regulators of mitochondrial-mediated apoptotic induction and act as either activators (Bax, Bad, Bak, and Bok) or inhibitors (Bcl-2, Bcl-xL, and Bcl-w).[23] As shown in Figure 3B, the exposure of HSC-3 cells to FKB caused a dramatic reduction in the levels of Bcl-2, a potent cell death inhibitor, and increased the levels of Bax protein, which heterodimerizes with Bcl-2 and inhibits Bcl-2 activity. In addition to the classic caspase-mediated apoptosis, mammalian cells can undergo caspase-independent apoptosis that is mediated by mitochondrial membrane permeability followed by apoptosis-inducing factor (AIF) release.[24] In addition to FKB-induced changes in mitochondrial membrane potential, a significant decrease in AIF was observed (Figure 3B). Taken together, these data suggest that FKB-induced apoptosis is mediated by both caspase-dependent and caspase-independent mechanisms.

FKB Activates Fas-Mediated Apoptosis through the Activation of Caspase-8. Upon ligand binding, death receptors trigger apoptosis through the activation of caspase-8-mediated apoptotic cascades. To assess whether FKB promotes apoptosis via a death receptor-mediated pathway, the expression levels of Fas and FasL were detected in HSC-3 cells by Western blot analysis. As shown in Figure 3C, FKB caused a significant dose-dependent induction of Fas expression. In sharp contrast, treatment of cells with FKB caused an increase in the expression of FasL protein at lower concentration (1.25 μg/mL), whereas sustained reductions in FasL expression were observed at >2.5 μg/mL of FKB. We reasoned that concentrations of FKB above 2.5 μg/mL may rapidly convert the membrane bound FasL (40 kDa) into soluble FasL (26 kDa). Therefore, the detectable amount of 40 kDa membrane bound FasL was dose-dependently reduced (converted) by FKB (Figure 3C). In addition, we also observed that FKB treatment significantly activated the downstream death receptor cascade, as evidenced by the reduction in procaspase-8 (44 kDa) levels in the cytoplasm, which may further amplify the mitochondrial membrane permeability. Taken together, these results strongly suggest that FKB also induces apoptosis of HSC-3 cells through the Fas/FasL-mediated death receptor pathway.

ER Stress Is Involved in FKB-Induced HSC-3 Cell Apoptosis. Recently, prolonged ER stress has been shown to result in apoptosis. To demonstrate the role of ER stress in FKB-induced apoptosis, HSC-3 cells were incubated with a specific ER tracking marker. ER-Tracker Green reagent is conjugated with glibenclamide, which binds the sulfonylurea receptors found in large concentrations on the endoplasmic reticulum. Therefore, ER-Tracker Green reagent provides highly selective ER labeling in living cells. The ER-Tracker green fluorescence in control cells was observed in perinuclear areas and in the cytoplasm, consistent with endoplasmic reticulum localization, whereas cells treated with FKB (>5 μg/mL) showed a heterogeneous distribution of green fluorescence (Figure 3A).

Several mechanisms have been proposed for linking ER stress to apoptosis, including activation of ER-associated caspases, especially caspase-4 in human and caspase-12 in mice.[25] Western blot analysis showed that FKB treatment for 24 h appeared to increase the activation of caspase-4 and caspase-12, as evidenced by the reduction of procaspase-4 (43 kDa) and procaspase-12 (55 kDa) in HSC-3 cells (Figure 3D). Eukaryotes react rapidly to ER stress through protective ER-resident stress proteins, such as heat shock proteins HSP70 and HSP90, to reestablish normal function. Therefore, the induction of heat shock proteins is a molecular marker of ER-stress. We also observed that FKB treatment significantly augmented the expression of ER chaperons, such as HSP70, in a dose-dependent manner (Figure 3D). Therefore, we conclude that ER stress induced by FKB may also play an important role in FKB-induced HSC-3 cell apoptosis.

FKB Treatment Induces Intracellular ROS Generation in HSC-3 Cells. ROS generation has been implicated as an early event in apoptosis. To determine whether FKB-induced apoptosis is ROS-dependent, cells were incubated with 5 μg/mL of FKB for 1−60 min before fluorescence microscopy analysis. shown in Figure 4A, rapid generation of ROS was detected at 1 min following FKB treatment, with a value 260% above that in control cells, whereas FKB treatment for 5, 10, 30, and 60 min caused a time-dependent decrease in the increased ROS generation to 190%, 165%, 140%, and 132%, respectively, compared with control cells (100%; $p < 0.05$). These data suggest that FKB treatment induces an early increase in intracellular ROS generation that could be an event upstream of changes in mitochondrial membrane potential and caspase activation.

FKB Activates Oxidative Stress-Related Proteins in Response to ROS Generation. The results described above suggested that FKB-induced apoptosis is mediated by ROS generation and ER stress. Therefore, we sought to examine whether oxidative stress-related proteins, such as HO-1 and Nrf2, are induced in FKB-treated HSC-3 cells. The inducible isoform of HO-1 effectively counteracts oxidative stress. Immunoblotting and immunofluorescence assays showed that HO-1 protein expression was faintly detected in control cells, a 5-fold induction in HO-1 expression was observed upon treatment with 5 μg/mL of FKB for 24 h, and a further 10-fold increase was observed upon treatment with 7.5 μg/mL of FKB. In contrast, a significant 2-fold decrease in the HO-1 protein level was observed upon treatment with 10 μg/mL of FKB, suggesting that higher concentrations of FKB may have irreversible cytotoxic effects on HSC-3 cells (Figure 4B,C). Nrf2 is a bZIP transcription factor that is responsible for ARE-dependent HO-1 transcription. Therefore, we examined whether FKB induced Nrf-2 activation. Compared with the control, FKB significantly increased the Nrf2 protein levels as measured by Western blot analysis (Figure 4B). A sustained increase in the nuclear Nrf2 expression was observed upon treatment with 2.5 μg/mL of FKB, gradually decreased to the basal level at 7.5 μg/mL, and was completely abolished at 10 μg/mL of FKB. We reasoned that the reduction in nuclear Nrf2 at higher concentrations of FKB may rapidly induce Nrf-2 transcriptional activation. Moreover, cytoplasmic Nrf2 was significantly reduced by 0.7-fold and 0.5-fold at 7.5 and 10 μg/mL of FKB, respectively (Figure 4B). In addition, total cell lysates exhibits increased Nrf2 turnover in a dose-depended manner, which strongly supports the notion that FKB induces oxidative stress in HSC-3 cells.

NAC Pretreatment Prevents FKB-Induced Apoptosis in HSC-3 Cells. To elucidate whether ROS generation is directly associated with FKB-induced mitochondrial dysfunction
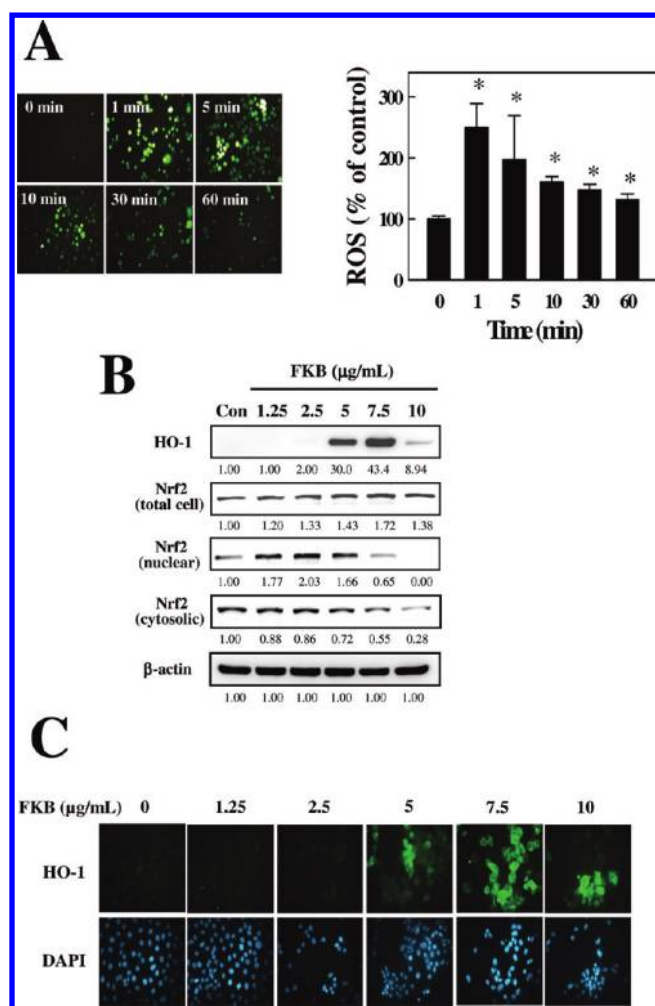
Figure 4. (A) Effects of FKB on intracellular ROS generation in HSC-3 cells. Cells were treated with FKB (7.5 μg/mL) for 0, 1, 5, 10, 30, and 60 min. The nonfluorescent cell membrane-permeable probe DCFH-DA (10 μM) was added to the culture medium 30 min before the end of each experiment. DCFH-DA permeable to cell membrane reacts with cellular ROS and is metabolized into fluorescent DCF, acting as an indicator of ROS that was measured by fluorescence microscopy (200× magnification). The intracellular ROS level, as a percentage of the control, is expressed in the graph. (B) The effects of FKB (1.25−10 μg/mL, 24 h) on the induction of HO-1 and Nrf2 in HSC-3 cells were measured by Western blotting. Protein (50 μg) from each sample was resolved by 8−15% SDS−PAGE with β-actin as a control. (C) Effect of FKB (1.25−10 μg/mL, 24 h) on HO-1 expression in HSC-3 cells was detected by an immunofluorescence assay using the appropriate antibodies. The cells were stained with DAPI (1 μg/mL) for 5 min and examined by fluorescence microscopy (magnification ×300).

and apoptosis, we examined ROS generation and mitochondrial membrane potential in HSC-3 cells preincubated with NAC (2.5 mM) for 1 h followed by treatment with FKB (7.5 μg/mL) for 1−5 min. As expected, NAC treatment significantly ($p < 0.05$) inhibited FKB-induced ROS generation (Figure 5A). Consequently, FKB-induced cell death was significantly ($p < 0.05$) prevented by NAC (Figure 5B). For example, compared with control, the percentage of cell viability significantly decreased to 40 ± 3% treatment upon treatment with FKB for 24 h, whereas the cell viability increased to 60 ± 5% upon pretreatment with NAC (Figure 5B). Furthermore, the
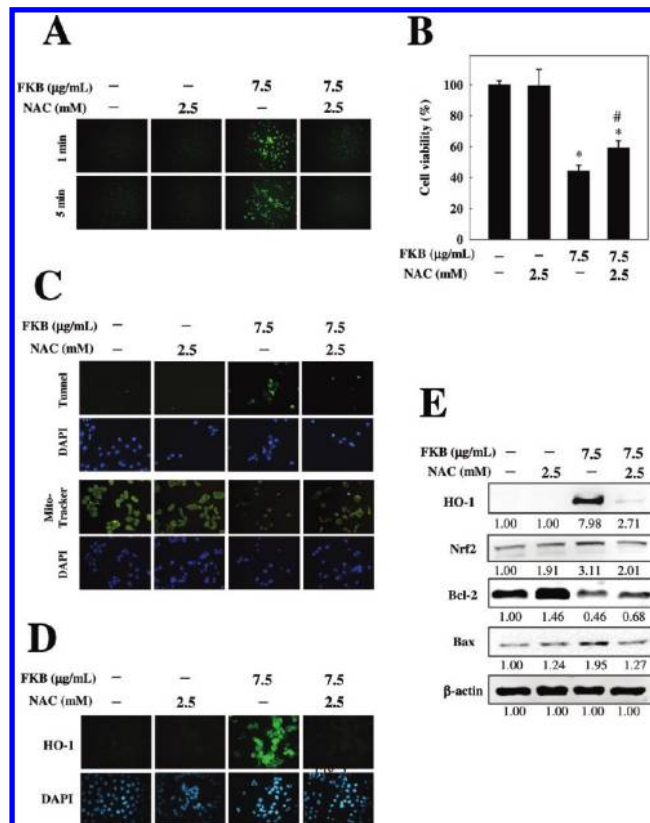

Figure 5. FKB-induced ROS generation is involved HSC-3 apoptosis. (A) Cells were pretreated with a 2.5 mM concentration of the antioxidant N-acetylcysteine (NAC) for 1 h followed by incubation with or without FKB (7.5 μg/mL) for 1−5 min, and the intracellular ROS generation was measured using the DCFH-DA fluorescence method. (B) The cell viability was determined by MTT assay as described in Materials and Methods. (C) Apoptosis induction was determined by TUNEL, and mitochondrial membrane potential was measured by Mito-Tracker assays as described in Materials and Methods. (D) HO-1, Nrf2, Bcl-2, and Bax proteins levels were monitored by Western blot analysis as described in Materials and Methods. The photomicrographs shown here are from one representative experiment that was repeated three times with similar results. Each value is expressed as the mean ± SD ($n = 3$). *,#Significant difference compared with control and FKB-treated group ($p < 0.05$).

TUNEL and Mito-Tracker fluorescence assays indicated that FKB treatment resulted in a profound DNA fragmentation and mitochondrial injury (Figure 5C), whereas NAC pretreatment significantly prevented the FKB-induced apoptotic DNA fragmentation and mitochondrial dysfunction in HSC-3 cells (Figure 5C). The immunofluorescence assay showed that pre-incubation with NAC caused a significant decrease in the FKB-induced HO-1 induction (Figure 5D). Figure 5E also shows that pretreatment with NAC significantly decreased the FKB-mediated HO-1/Nrf2 induction and Bax/Bcl-2 dysregulation. These results confirm that FKB-induced ROS generation might involve mitochondrial-mediated apoptosis in human oral carcinoma HSC-3 cells.

FKB Inhibits Phosphorylation of PI3K/Akt in HSC-3 Cells. The PI3K/Akt signaling pathway and its downstream transcription factors have been extensively studied for their role in cell proliferation, survival, cell-cycle control, and other cellular functions.[26] Indeed, the dysregulation of the PI3K/Akt signaling pathway leads to tumorigenesis in vitro and in vivo.[27]

We therefore investigated whether FKB treatment could affect the activation of PI3K/Akt by assessing phosphorylation of Akt and its direct upstream kinase PI3K in cells that were incubated with 1.25−10 μg/mL of FKB for 0.5−24 h. Western blot analysis showed that FKB treatment significantly inhibited the activation of Akt as shown by a decrease in the phosphorylation of Akt in a dose- and time-dependent manner (Figure 6A). Also, FKB decreased total Akt expression in a dose- and time-
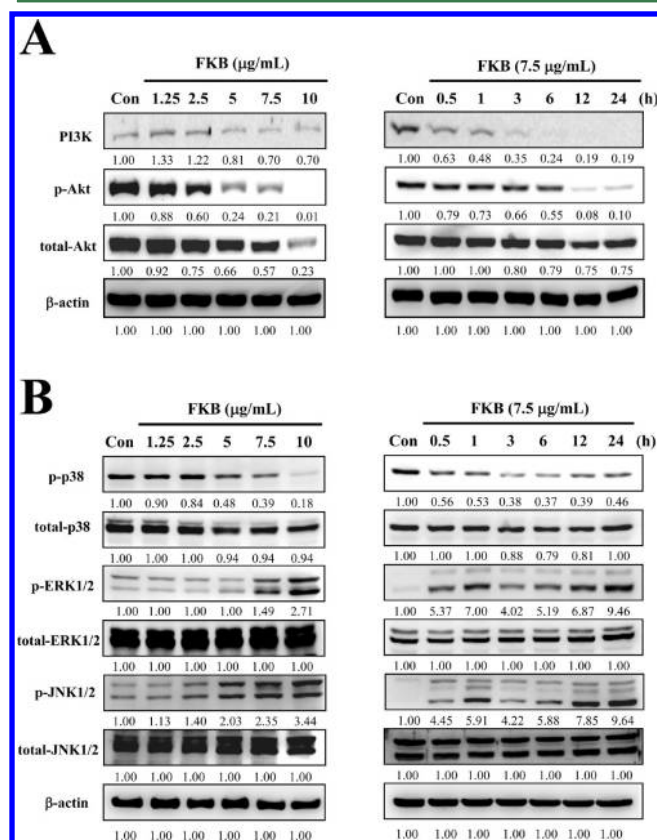
Figure 6. FKB downregulates PI3K/Akt and p38 MAPK and upregulates JNK1/2 and ERK1/2 activation in HSC-3 cells. (A) Western blot analysis shows that FKB treatment suppressed the phosphorylation of Akt and p38 and enhanced the phosphorylation of ERK1/2 and JNK1/2 in HSC-3 cells. Cells were treated with 1.25−10 μg/mL FKB for 24 h or with 7.5 μg/mL FKB for 0.5−24 h, and the levels of phosphorylated Akt (p-Akt), p38 (p-p38), ERK1/2 (p-ERK1/2), and JNK1/2 (p-JNK1/2) were evaluated using phosphorylation-specific antibodies against Akt, p38, ERK1/2, or JNK1/2 by Western blot analysis. Total Akt, p38, ERK1/2, or JNK1/2 levels were assessed as the loading controls. The levels of the indicated proteins in the cell lysates were analyzed using specific antibodies, and the amounts of β-actin were used as internal controls for sample loading. The photomicrographs shown here are from one representative experiment repeated twice with similar results. The results are presented as the mean ± SD of three assays. *Significant difference compared with the control group ($p < 0.05$).

dependent manner (Figure 6A). In contrast, phosphorylated PI3K levels were undetectable in HSC-3 cells. In addition, the total PI3K protein levels were significantly inhibited in response to FKB treatment (Figure 6A).

FKB Treatment Downregulates p38 MAPK and Upregulates ERK and JNK Proteins in HSC-3 Cells. In light of the evidence that MAP kinase family proteins, including p38, ERK, and JNK, play a critical role in cell fate,[28] the effects of FKB on the expression and activation of MAPKs was

examined. HSC-3 cells were treated with 1.25−10 μg/mL of FKB for 0.5−24 h, and the phosphorylation of p38, ERK, and JNK was assessed by Western blot analysis. As shown in Figure 6B, FKB significantly inhibited the activation of p38 MAPK in a dose- and time-dependent manner, and FKB (10 μg/mL) nearly completely inhibited the phosphorylation of p38 MAPK. However, FKB did not change the expression levels of p38 MAPK. In contrast, FKB treatment resulted in a 1.47- and 2.7-fold increase in ERK1/2 activity at 5 μg/mL and 10 μg/mL, respectively (Figure 6B). In addition, a 2-, 2.3-, and 3.4-fold increase in the phosphorylation of JNK1/2 resulted from FKB treatment at 2.5, 5, 7.5, and 10 μg/mL, respectively (Figure 6B). Similarly, FKB induced the phosphorylation of ERK in a time-dependent manner. A 7-fold induction in phosphorylation of ERK1/2 was observed at 1 h; this activation diminished at 3 h, then continued 9.4-fold at 24 h. JNK1/2 was also maximally phosphorylated at 1, 12, and 24 h as demonstrated by a 5.91-, 7.85-, and 9.64-fold induction in phosphorylation, respectively (Figure 5B). However, neither ERK1/2 nor JNK1/2 expression levels were affected by FKB treatment.

FKB Mediated Inactivation of PI3K/Akt Plays a Functional Role in G$_2$/M Arrest and Apoptosis in HSC-3 Cells. The PI3K/Akt signaling pathway is known to be involved in cell-cycle regulation, proliferation, and survival. To further determine whether the FKB-mediated inhibition of G$_2$/M arrest and apoptosis occurred mainly through the suppression of the Akt signaling pathway, HSC-3 cells were pretreated with an Akt-specific inhibitor (LY294002) for 1 h followed by treatment with FKB for 24 h. The results from the MTT assay demonstrated that a single treatment of FKB (2.5 μg/mL) or LY294002 (30 μM) reduced cell viability by 91.0 ± 1.8% and 63.2 ± 2.8%, respectively. The cell viability was further reduced to 45.8 ± 5.1% ($p < 0.05$) upon combination treatment with FKB and LY294002 for 24 h (Figure 7A). We next sought to examine whether pharmacological inhibition of Akt could enhance G$_2$/M cell-cycle arrest and apoptosis. The cells were incubated with a 2.5−10 μM concentration of the Akt-specific inhibitor LY294002 for 24 h, and the major G$_2$/M cell-cycle check point and apoptotic proteins were measured by Western blot analysis. As shown in Figure 7B, treatment of HSC-3 cells with the Akt inhibitor LY294002 let to concentration-dependent decrease in cell-cycle regulatory proteins, including cyclin A, cyclin B, Cdc2, and Cdc25C. The reduction in cell viability following LY294002 treatment was significantly associated with apoptosis, as shown by the activation of caspase cascades, including caspase-3, caspase-4, caspase-8, caspase-9, and caspase-12 and the inhibition of Bcl-2 (Figure 7C). These results clearly demonstrated that pharmacological inhibition of PI3K/Akt could induce G$_2$/M cell-cycle arrest and apoptosis, as evidenced by downregulation of cell-cycle regulatory proteins and upregulation of the apoptosis cascade. Taken together, these data suggest that inhibition of PI3K/Akt activity using a pharmacological approach enhances FKB-induced apoptosis and cell-cycle arrest in human oral carcinoma.

Suppression of the p38 MAPK Signaling Pathway Is Involved in FKB-Induced G$_2$/M Arrest and Apoptosis in HSC-3 Cells. p38 MAPK has been demonstrated to play a major role in cell survival, proliferation, differentiation, and apoptosis in mammalian cells.[29] To determine whether p38 MAPK is involved FKB mediated cell-cycle arrest and apoptosis, HSC-3 cells were preincubated with a pharmacological inhibitor of p38 MAPK (SB203580) for 1 h followed by treatment of FKB for 24 h. Figure 7A shows that a single treatment of FKB

2392

dx.doi.org/10.1021/jf205053r | J. Agric. Food Chem. 2012, 60, 2385−2397
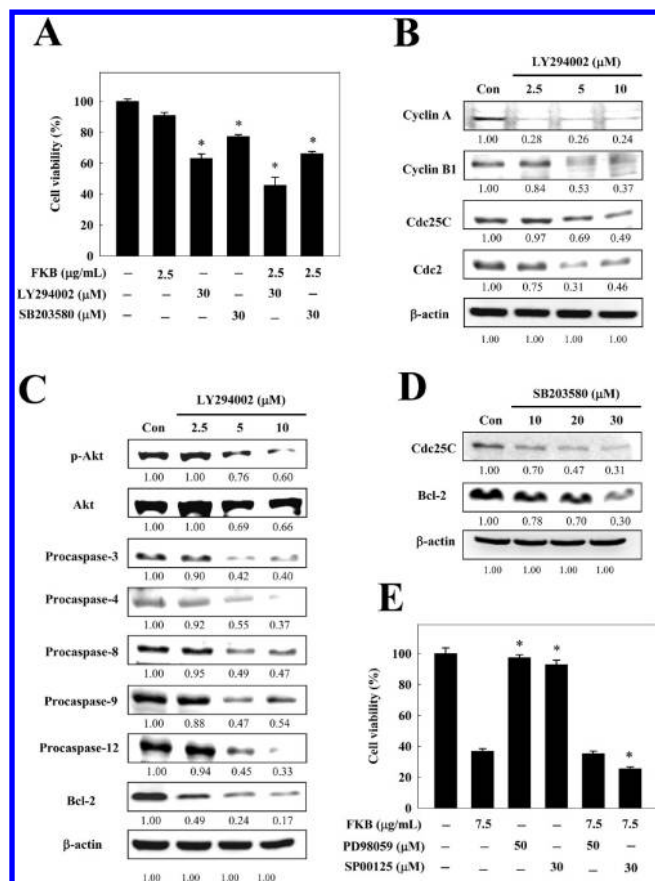
Figure 7. FKB mediates G_2/M arrest and apoptosis by inactivating the Akt signaling pathways. HSC-3 cells were pretreated with an Akt inhibitor (LY294002; 10, 20, or 30 μM) or p38 inhibitor (SB203580; 10, 20, or 30 μM) for 1 h and then treated with or without 2.5 $\mu g/mL$ FKB for 24 h; the effects on G_2/M arrest and apoptosis were evaluated by cell viability (A) and Western blotting (B–D) as described in Materials and Methods. Immunoblotting against p-Akt, Akt, caspase-3, caspase-4, caspase-8, caspase-9, caspase-12, Bcl-2, Bax, cyclin A, cyclin B1, Cdc2, and Cdc25C was performed. Each value is expressed as the mean ± SD ($n = 3$). (E) HSC-3 cells were pretreated with an ERK inhibitor (PD98059; 50 μM) or JNK inhibitor (SP600125; 30 μM) for 1 h and then treated with or without 7.5 $\mu g/mL$ FKB for 24 h; the effects on the cell viability was evaluated by MTT assay as described in Materials and Methods. *$p < 0.05$ is the FKB or inhibitor-treated groups compared with the control.

(2.5 $\mu g/mL$) or SB203580 (30 μM) reduced the cell viability by 91.0 ± 1.8% and 77.2 ± 1.3%, respectively, and the combination treatment (SB203580 and FKB) reduced the cell viability even more dramatically by 66.2 ± 1.4% ($p < 0.05$). Western blot analysis also showed that treatment with 10–30 μM SB203580 for 24 h dose-dependently attenuated the expression of the G_2/M cell-cycle regulatory kinase Cdc25C and the antiapoptotic Bcl-2 in HSC-3 cells (Figure 7D). Therefore, we concluded that the inactivation of p38 MAPK may be involved in FKB-induced cell-cycle arrest and/or apoptosis.

However, neither the ERK nor JNK inhibitor (PD98059 nor SP600125) showed a protective effect against FKB-induced cell death in HSC-3 cells (Figure 7E). Western blot analysis and TUNEL assays also demonstrated that ERK and JNK inhibitors failed to modulate G_2/M arrest and apoptotic regulatory proteins in HSC-3 cells (data not shown). Thus, these data clearly demonstrate that ERK and JNK activation is not involved in FKB-induced cell-cycle arrest and apoptosis in HSC-3 cells.

DISCUSSION

Oral cancer is the leading cause of cancer-related deaths in Taiwan, India, and South Asian countries. Therefore, the development of effective chemopreventive or chemotherapeutic agents is highly warranted to address this issue. Currently, many reports have emphasized that use of dietary bioactive compounds is becoming an alternative, safe and striking approach to control and treat cancer. Chalcones (one of the major classes of naturally occurring biological compounds with widespread distribution in fruits, vegetables, spices, tea, and soy-based foodstuffs) have recently been gaining much attention for their interesting pharmacological applications.[30] Several epidemiological studies have shown that chalcones present in cruciferous vegetable are protective against several human malignancies.[31] In the present study, we have evaluated the chemopreventive effects of FKB, a naturally occurring chalcone isolated from the rhizomes of *Alpinia pricei* (shell gingers), against human oral carcinoma HSC-3 cells in vitro. Previous studies have shown that FKB exhibits cytotoxic potency against human colon (HCT-116), lung adenocarcinoma epithelial (A-549), prostate (PC3 and DU-145), and squamous carcinoma (KB) cell lines.[16,19,32] We found that FKB also has significant cytotoxic effects against human oral carcinoma (HSC-3), oral adenosquamous carcinoma (Cal-27), melanoma (A-2058), and lung adenocarcinoma epithelial (A-549) cell lines. A profound cytotoxic effect of FKB was observed in HSC-3 cells compared with Cal-27, A-2058, and A-549. Here, we describe the mechanism through which FKB induces G_2/M cell-cycle arrest and apoptosis of human oral carcinoma HSC-3 cells. We initially found that FKB treatment had a profound effect on cell-cycle progression, evidenced by an increased population of cells in G_2/M phase. FKB decreased cyclin A and cyclin B protein levels with a concomitant decrease in the kinase Cdc2 activity in HSC-3 cells. Furthermore, FKB was able to suppress Cdc2 activity through the downregulation of Cdc25C, thus controlling the entry of cells into mitosis by maintaining the G_2/M transition phase. These data revealed that FKB-induced G_2/M arrest and inhibition of cyclin A/B was achieved through the downregulation of Cdc2/Cdc25C in HSC-3 cells. These data are in agreement with our previous study that suggested that FKB induces G_2/M cell-cycle arrest in human squamous carcinoma KB cells.[19] Notably, flavokawain A, a close analogue of FKB in kava extracts, increases the expression of p21/WAF1 and p27/KIP1 proteins, which results in a decrease in cyclin-dependent kinase 2 (CDK2) activity and subsequent G_1 cell-cycle arrest in the p53 wild type bladder cancer RT4 cell line. Flavokawain A also induced a G_2/M arrest in six p53 mutant bladder cancer cell lines.[33] Interestingly, HSC-3 cells also have mutations causing a C-terminal truncation of the p53 protein.[34] However, HSC-3 cells display a stronger response to FKB treatment than A549 cells, which have wild type p53.

FKB not only induced cell-cycle arrest at the G_2/M boundary but also caused apoptotic cell death of human oral carcinoma HSC-3 cells through the mitochondrial-mediated pathway as evidenced by mitochondrial cytochrome *c* release, activated caspase-3, caspase-9, and PARP cleavage and dysegulation of the Bax/Bcl-2 ratio. Other researchers have found that the mechanisms through which FKB induces apoptosis depended primarily on mitochondrial damage,[17] GSH-sensitive oxidative stress,[35] upregulation of Bim and death receptors,[16] and generation of ROS and GDD153-mediated mitochondrial membrane depolarization.[32] Several lines of evidence have suggested that caspase-independent apoptosis can occur based on studies involving an irreversible loss of mitochondrial function and those

demonstrating mitochondrial release of caspase-independent death effectors, including AIF and EndoG.[36] Our study showed that treatment of HSC-3 cells with FKB induced a dose-dependent decrease in AIF expression. Taken together, the data in the present study suggest that FKB-induced apoptosis is mediated by both caspase-dependent and caspase-independent mechanisms.

Investigations have shown that apoptosis is controlled by both mitochondrial and membrane death receptor pathways. The extrinsic pathway is initiated by the binding of trans-membrane death receptors, including Fas, FasL, TNFR1, and TRAIL receptors with cognate extracellular ligands.[37] A recent report has demonstrated that chalcones transiently enhance death ligand-mediated apoptosis in various cancer cell lines.[38] Cross-talk exists between the extrinsic and intrinsic pathways; activated caspase-8 can cleave Bid to produce truncated Bid (t-Bid), which then binds to mitochondria and promotes mito-vchondrial membrane integrity.[39] Previously, we have also shown that treatment of human squamous carcinoma KB cells with FKB results in apoptosis through death-receptor and mitochondrial pathways, while these effects were not observed in normal human gingival fibroblast HGF cells.[19] These reports prompted us to further examine whether the death receptor pathway is also involved in FKB-induced apoptosis in HSC-3 cells. We found that FKB enhances death receptor-induced apoptosis in HSC-3 cells. This conclusion was supported by following evidence that FKB activated caspase-8 and induced Fas/FasL expression in HSC-3 cells.

ER stress-induced apoptosis has its own signaling pathway. The precise molecular mechanism of ER stress-induced apoptosis still poorly understood.[40] Bcl-2 family proteins are localized in the ER membrane and have been shown to influence ER homeostasis and membrane permeability.[41] This pathway is independent of mitochondria and death receptors and is thought to be mediated by caspase-12.[40] Stimulated caspase-12 reportedly further activates caspase-9 independent of Apaf-1, followed by activation of caspase-3.[25] As an alternative to caspase-12 in human, caspase-4 is involved in the ER stress-induced cell death pathway. Both murine caspase-12 and human caspase-4 are localized to the ER and are cleaved specifically by ER stress.[25] Our data supports the notion that FKB-induced apoptosis is mediated by the ER stress pathway as evidenced by the increased activation of Bax and caspase-4 and caspase-12 in HSC-3 cells. These results also imply that FKB influences an additional apoptotic pathway that functions independently of the release of mitochondrial proteins.

Many anticancer drugs have been suggested to generate ROS, which causes oxidative stress-induced apoptosis in cancer cells, while many inhibitors of apoptosis show antioxidant activity.[42] Indeed, factors that cause or promote oxidative stress, such as ROS production, lipid peroxidation, downregulation of antioxidant defenses characterized by reduced glutathione levels, and reduced transcription of superoxide dismutase, catalase, and thioredoxin, have been shown to be involved in apoptotic processes.[11] Kuo et al. have reported that the generation of ROS acts as an important cellular event induced by FKB and results in mitochondrial-dependent apoptosis in human colon cancer cells.[32] In agreement with a previous report,[32] our current data also demonstrate that FKB remarkably increased intracellular ROS accumulation in human oral cancer HSC-3 cells.

ROS have been shown to induce oxidative stress in a variety of organisms. When oxidative stress is triggered, cells are able to maintain a state of redox homeostasis. This equilibrium can only be activated by a cellular antioxidant defense system. The induction of HO-1 represents a key defense mechanism against cellular oxidative stress. Previous studies have demonstrated that Nrf2/ARE-mediated HO-1 expression is induced by a variety of plant-derived polyphenols.[43] In this study, a significant increase in HO-1 expression was associated with FKB treatment. The mechanism of HO-1 induction by FKB was observed to be by ROS production, which activated nuclear translocation of Nrf2, a transcription factor that binds to ARE in the HO-1 promoter region. It is worthy to note that HO-1 protein expression was almost undetectable in control cells. Our data are also consistent with the notion that the activation of HO-1 by FKB in HSC-3 cells required ROS generation because pharmacological inhibition of ROS using the antioxidant NAC significantly reduced HO-1 and Nrf2 protein levels, whereas HO-1/Nrf2 expression levels were reversible in response to FKB treatment. This result is consistent with previous observations in which the expression of HO-1/Nrf2 has been thought to be a cellular defense mechanism against ROS-induced oxidative stress in HSC-3 cells.[44]

Akt, a serine/threonine kinase, is recruited to the cell membrane by PI3K, which blocks apoptosis in a variety of cells.[45] Conversely, the inhibition of PI3K/Akt activation may result in cell growth arrest and apoptosis.[46] Kumar et al. have reported that combination treatment with cisplatin and a PI3K inhibitor (LY294002) results in a significant apoptotic effect against oral squamous cell carcinoma (OSCC-3) and endothelial cells compared with each agent used alone.[47] To test this phenomenon, we performed combination treatment studies with FKB and various inhibitors, including PI3K (LY294002), p38 MAPK (SB203580), ERK (PD98059), and JNK (SP600125) inhibitors which by themselves did not show very significant inhibition of HSC-3 survival. Combination treatment with FKB and LY294002/SB203580 significantly decreased HSC-3 cell survival and induced apoptosis, whereas the combination of FKB with ERK and JNK inhibitors failed to show any significant inhibition of HSC-3 survival. In addition, the combination of FKB with LY294002 showed a significantly higher level of inhibition of HSC-3 cell survival compared with the combination of FKB and SB203580.

The critical role of MAPK family proteins in cell proliferation and apoptosis is well characterized by the observation that dysregulation of these kinase cascades can result in cell transformation and cancer.[28] The p38 MAPK has recently gained attention as a tumor suppresser that is activated upon cellular stress and often engages pathways that can block proliferation or promote apoptosis.[48] However, p38 MAPK has been shown to induce apoptosis in some cells but prevent apoptosis in others.[49] Our results indicated that the p38 MAPK inhibitor SB203580 reduced HSC-3 survival and caused the downregulation of a cell-cycle regulatory protein (Cdc25C) and antiapoptotic protein (Bcl-2). These data correlate with others' observations that p38 MAPK inhibitors block tumor cell growth by modulating the activity of Cdc25 phosphatases[50] and decreasing the expression of Bcl-2.[28] Therefore, we concluded that the inactivation of p38 MAPK may be involved in FKB-induced cell-cycle arrest and/or apoptosis in HSC-3 cells.

The ERK pathway primarily directs a program of proliferation and survival, while the JNK pathway cannot promote either proliferation or apoptosis. Transient activation of ERK and JNK leads to increased proliferation and survival of cancer cells, although inactivation of JNK in some instances may also
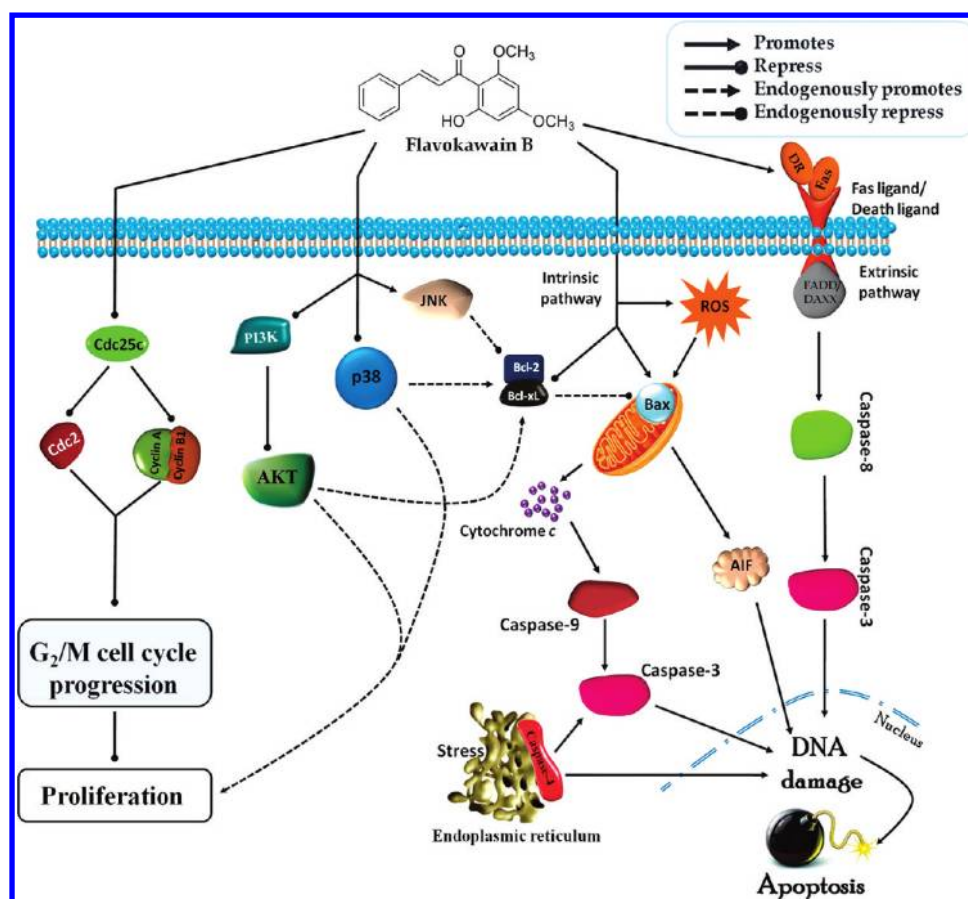
Figure 8. Proposed diagrams of FKB-induced G_2/M arrest and apoptosis via ROS generation and Akt/p38 MAPK inactivation in human oral carcinoma HSC-3 cells.

promote tumorigenesis.[28] We found that FKB significantly enhanced the activation of ERK and JNK, but no significant modulation of cell survival, G_2/M arrest, and apoptotic induction was observed in cells pretreated with the ERK or JNK inhibitors, PD98059 or SP600125, respectively. These findings indicate that activation of JNK and ERK is not involved in FKB-induced cell-cycle arrest and/or apoptosis in HSC-3 cells.

The mechanisms by which FKB induces G_2/M arrest and apoptosis through ROS generation and Akt/p38 MAPK inactivation in HSC-3 cells are summarized in Figure 8. Indeed, the induction of apoptosis by FKB is associated with mitochondrial, death receptor, and ER stress-induced pathways. These data provide an important new insight into the possible molecular mechanisms of FKB and its promising potential as a chemopreventive agent against human oral cancer. Further in vivo studies are required to confirm whether FKB represents an effective chemotherapeutic agent for the management of oral cancers.

■ AUTHOR INFORMATION

Corresponding Author

*Phone: +886-4-22053366x7503. Fax: +886-4-22062891. E-mail: hlyang@mail.cmu.edu.tw; charaljana14@rediffmail.com.

Notes

The authors declare no competing financial interest.

■ ABBREVIATIONS USED

ROS, reactive oxygen species; PARP, poly(ADP-ribose) polymerase; HO-1, hemeoxygenase-1; Nrf2, NF-E2-related factor-2; NAC, N-acetyl-L-cysteine; PI3K, phosphatidylinositol 3-kinase; MAPK p38, mitogen-activated protein kinase p38; JNK, c-jun N-terminal kinase; ERK, extracellular signal-regulated protein kinase; Cdc25C, cell division cycle 25C

■ REFERENCES

(1) Hsu, S.; Sing, B.; Schuster, G. Induction of apoptosis in oral cancer cells: agents and mechanisms for potential therapy and prevention. *Oral Oncol.* **2004**, *40*, 461–473.

(2) Ahluwalia, K. P. Assessing oral cancer risk of South-Asian immigrants in New York City. *Cancer* **2005**, *104*, 2959–2961.

(3) Ahmad, N.; Adhami, V. M.; Afaq, F.; Feyes, D. K.; Mukhtar, H. Resveratrol causes WAF-1/p21-mediated G1-phase arrest of cell cycle and induction of apoptosis in human epidermoid carcinoma A431 cells. *Clin. Cancer. Res.* **2001**, *7*, 1466–1473.

(4) Hseu, Y. C.; Chen, S. C.; Chen, H. C.; Liao, J. W.; Yang, H. L. *Antrodia camphorata* inhibits proliferation of human breast cancer cells *in vitro* and *in vivo*. *Food Chem. Toxicol.* **2008**, *46*, 2680–2688.

(5) Bloom, J.; Cross, F. R. Multiple levels of Cyclin specificity in cell-cycle control. *Nat. Rev. Mol. Cell Biol.* **2007**, *8*, 149–160.

(6) Giansanti, V.; Scovassi, A. I. Cell death: A one-way journey to the graveyard. *Open Biol. J.* **2008**, *1*, 27–34.

(7) Lin, C. T.; Kumar, K. J. S.; Tseng, Y. H.; Wang, Z. J.; Pan, M. Y.; Xiao, J. H.; Chien, S. C.; Wang, S. Y. Anti-inflammatory activity of

2395

dx.doi.org/10.1021/jf205053r | *J. Agric. Food Chem.* 2012, 60, 2385–2397

flavokawain B from *Alpini pricei* Hayata. *J. Agric. Food. Chem.* **2009**, *57*, 6060−6065.

(8) Chen, I. N.; Chang, C. C.; Ng, C. C.; Wang, C. Y.; Shyu, Y. T.; Chang, T. L. Antioxidant and antimicrobial activity of Zingiberaceae plants in Taiwan. *Plant Foods Hum. Nutr.* **2008**, *63*, 15−20.

(9) Srividhya, A. R.; Dhanabal, S. P.; Misra, V. K.; Suja, G. Antioxidant and antimicrobial activity of *Alpinia officinarum*. *Ind. J. Pharm. Sci.* **2010**, *72*, 145−148.

(10) Lee, J.; Kim, K. A.; Jeong, S.; Lee, S.; Park, H. J.; Kim, N. J.; Lim, S. Antiinflammatory, antinociceptive and antipsychiatric effects by the rzhizomes of *Alpinia officinarum* on complete Freund's adjuvant-induced arthritis in rats. *J. Ethnopharmacol.* **2009**, *26*, 258−264.

(11) Yang, H. L.; Chen, S. C.; Chen, C. S.; Wang, S. Y.; Hseu, Y. C. *Alpinia pricei* rhizome extracts induce apoptosis of human carcinoma KB cells via a mitochondria-dependent apoptotic pathway. *Food. Chem. Toxicol.* **2008**, *46*, 3318−3324.

(12) Hsu, C. L.; Yu, Y. S.; Yen, G. C. Anticancer effects of *Alpinia pricei* Hayata roots. *J. Agric. Food. Chem.* **2010**, *58*, 2201−2208.

(13) Bendjeddou, D.; Lalaoui, K.; Satta, D. Immunostimulating activity of the hot water-soluble polysaccharide extracts of *Anacyclus pyrethrum*, *Alpinia galangal* and *Citrullus colocynthis*. *J. Ethnopharmacol* **2003**, *88*, 155−160.

(14) Kadota, S.; Tezuka, Y.; Prasain, J. K.; Ali, M. S.; Banskota, A. H. Novel diarylheptanoids of *Alpinia blepharocalyx*. *Curr. Top. Med. Chem.* **2003**, *3*, 203−225.

(15) Hseu, Y. C.; Chen, C. S.; Wang, S. Y. *Alpinia pricei* rhizome extracts induce cell cycle arrest in human squamous carcinoma KB cells and suppress tumor growth in nude mice. *eCAM* **2011**, DOI: 10.1093/ecam/nep142.

(16) Tang, Y.; Li, X.; Liu, Z.; Simoneau, A. R.; Xie, J.; Zi, X. Flavokawain B, a kava chalcone, induces apoptosis *via* up-regulation of death-receptor 5 and Bim expression in androgen receptor negative, hormonal refractory prostate cancer cell lines and reduces tumor growth. *Int. J. Cancer* **2010**, *127*, 1758−1768.

(17) Zi, X.; Simoneau, A. R. Flavokawain A, a novel chalcone from kava extract, induces apoptosis in bladder cancer cells by involvement of Bax protein-dependent and mitochondria-dependent apoptotic pathway and suppresses tumor growth in mice. *Cancer Res.* **2005**, *65*, 3479−3486.

(18) Steiner, G. G. The correlation between cancer incidence and kava consumption. *Hawaii Med. J.* **2000**, *59*, 420−422.

(19) Lin, E.; Lin, W. H.; Wang, S. Y.; Chen, C. S.; Liao, J. W.; Chang, H. W.; Chen, S. C.; Lin, K. Y.; Wang, L.; Yang, H. L.; Hseu, Y. C. Flavokawain B inhibits growth of human squamous carcinoma cells: Involvement of apoptosis and cell cycle dysregulation in vitro and *in vivo*. *J. Nutr. Biochem.* **2011**, DOI: 10.1016/j.jnutbio.2011.01.002.

(20) Joza, N.; Susin, S. A.; Daugas, E.; Stanford, W. L.; Cho, S. K.; Li, C. Y.; Sasaki, T.; Elia, A. J.; Cheng, H. Y.; Ravagnan, L.; Ferri, K. F.; Zamzami, N.; Wakeham, A.; Hakem, R.; Yoshida, H.; Kong, Y. Y.; Mak, T. W.; Zúñiga-Pflücker, J. C.; Kroemer, G.; Penninger, J. M. Essential role of the mitochondrial apoptosis-inducing factor in programmed cell death. *Nature* **2001**, *140*, 549−554.

(21) Yu, J.; Guo, Q. L.; You, Q. D.; Zhao, L.; Gu, H. Y.; Yang, Y.; Zhang, H. W.; Tan, Z.; Wang, X. Gambogic acid-induced G2/M phase cell-cycle arrest *via* disturbing CDK7-mediated phosphorylation of CDC2/p34 in human gastric carcinoma BGC-823 cells. *Carcinogenesis* **2007**, *28*, 632−638.

(22) Johnson, D. G.; Walker, C. L. Cyclins and cell cycle check points. *Annu. Rev. Immunol. Toxicol.* **1999**, *39*, 295−312.

(23) Gross, A. Bcl-2 proteins: Regulators of the mitochondrial apoptotic program. *IUBMB Life* **2001**, *52*, 231−236.

(24) Liang, H.; Salinas, R. A.; Leal, B. Z.; Kosakowska-Cholody, T.; Michejda, C. J.; Waters, S. J.; Herman, T. S.; Woynarowski, J M.; Woynarowska, B. A. Caspase-mediated apoptosis and caspase-independent cell-death induced by irofulven in prostate cancer cells. *Mol. Cancer Ther.* **2004**, *3*, 1385−1396.

(25) Shiraishi, H.; Okamoto, H.; Yashimura, A.; Yoshida, H. ER stress-induced apoptosis and caspase-12 activation occurs downstream of mitochondrial apoptosis involving Apaf-1. *J. Cell Sci.* **2006**, *119*, 3958−3966.

(26) Zhang, X.; Jin, B.; Huang, C. The PI3K/Akt pathway and its downstream transcriptional factors as targets for chemoprevention. *Curr. Cancer Drug Targets* **2007**, *7*, 305−316.

(27) Vivanco, I.; Sawyers, C. L. The phosphatidylinositol 3-kinase−Akt pathway in human cancer. *Nat. Rev. Cancer* **2002**, *2*, 489−501.

(28) Kennedy, N. J.; Cellurale, C.; Davis, R. J. A radical role for p38 MAPK in tumor initiation. *Cell* **2007**, *11*, 101−103.

(29) Zhang, W.; Liu, H. T. MAPK signal pathway in the regulation of cell proliferation in mammalian cells. *Cell Res.* **2002**, *12*, 9−18.

(30) Nowakowska, Z. A review of anti-infective and anti-inflammatory chalcones. *Eur. J. Med. Chem.* **2007**, *42*, 125−137.

(31) Orlikova, B.; Tasdemir, D.; Golais, F.; Dicato, M.; Diederich, M. Dietary chalcones with chemopreventive and chemotherapeutic potential. *Genes Nutr.* **2011**, *6* (2), 125−147.

(32) Kuo, Y. F.; Su, Y. Z.; Tseng, Y. H.; Wang, S. Y.; Wang, H. M.; Chueh, P. J. Flavokawain B, a novel chalcone from *Alpinia pricei* Hayata with potent apoptotic activity: Involvement of ROS and GADD153 upstream of mitochondria-dependent apoptosis in HCT116 cells. *Free Radical Biol. Med.* **2010**, *49*, 214−226.

(33) Tang, Y.; Simoneau, A. R.; Xie, J.; Shahandeh, B.; Zi, X. 2008. Effect of the kava chalcone flavokawain A differ in bladder cancer cells with wild-type versus mutant p53. *Cancer Prev. Res.* **2008**, *1*, 436−451.

(34) Ichwan, S. J. A.; Yamada, S. Y.; Sumrejkanchanakij, P.; Ibrahim-Auerkari, E.; Eto, K.; Ikeda, M.-A. Defect in serine 46 phosphorylation of p53 contributes to acquisition of p53 resistance in oral squamous cell carcinoma cells. *Oncogene* **2006**, *25*, 1216−1224.

(35) Zhou, P.; Gross, S.; Liu, J. H.; Yu, B. Y.; Feng, L. L.; Nolta, J.; Sharma, V.; Piwnica-Worms, D.; Qiu, S. X. Flavokawain B, the hepatotoxic constituent from kava root, induces GSH-sensitive oxidative stress through modulation of IKK/NF-κB and MAPK signaling pathways. *FASEB J.* **2010**, *24* (12), 4722−4732.

(36) Kroemer, G.; Galluzzi, L.; Brenner, C. Mitochondrial membrane permeabilization in cell death. *Physiol. Rev.* **2007**, *87*, 99−163.

(37) Azhkenazi, A. Targeting death and decoy receptors of the tumour necrosis factor superfamily. *Nat. Rev. Cancer* **2002**, *2*, 420−430.

(38) Szliszka, E.; Czuba, Z. P.; Mazur, B.; Sedek, L. Chalcones enhance TRAIL-induced apoptosis in prostate cancer cells. *Int. J. Mol. Sci.* **2010**, *11*, 1−13.

(39) Subramaniam, D.; Giridharan, P.; Murmu, N.; Shankarnarayanan, N. P.; May, R.; Houchen, C. W.; Ramanujam, R. P.; Balakrishnan, A.; Vishwakarma, R. A.; Anant, S. Activation of apoptosis by 1-hydroxy-5, 7-dimethoxy-2-naphthalene-carboxaldehyde (HDNC), a novel compound from *Aegle marmelos*. *Cancer Res.* **2008**, *68* (20), 8573−8581.

(40) Szegezdi, E.; Fitzgerald, U.; Samali, A. Caspase-12 and ER-stress-mediated apoptosis. The story so far. *Ann. N.Y. Acad. Sci.* **2003**, *1010*, 186−194.

(41) Breckenridge, D.; Germain, M.; Mathai, J.; Nguyen, M.; Shore, G. C. Regulation of apoptosis by endoplasmic reticulum pathways. *Oncogene* **2003**, *22*, 8608−8618.

(42) Lan, A. T. Y.; Wang, Y.; Chiu, J. F. Reactive oxygen species: Current knowledge and applications in cancer research and therapeutic. *J. Cell. Biochem.* **2008**, *104*, 657−667.

(43) Kim, J. W.; Li, M. H.; Jang, J. H.; Na, H. K.; Song, N. Y.; Lee, C.; Johnson, J. A.; Surh, Y. J. 15-Deoxydelta (12,14)-prostaglandin J_2 rescues PCl2 cells from H_2O_2-induced apoptosis through Nrf2-mediated up-regulation of heme oxygenase-1 potential roles of Akt and ERK1/2. *Biochem. Pharmacol.* **2008**, *76*, 1577−1589.

(44) Lee, H. Z.; Liu, W. Z.; Hsieh, W. T.; Tang, F. Y.; Chung, J. G.; Leung, H. W. C. Oxidative stress involement in *Physalis angulata*-induced apoptosis in human oral cancer cells. *Food Chem. Toxicol.* **2009**, *47*, 561−570.

(45) Page, C.; Lin, H. J.; Jin, Y.; Castle, V. P.; Nunez, G.; Huang, M.; Lin, J. Overexpression of Akt can modulate chemotherapy-induced apoptosis. *Anticancer Res.* **2002**, *20*, 404−416.

(46) Vega, F.; Medeiros, L. J.; Leventaki, V.; Atwell, C.; Cho-Vega, J. H.; Tian, L.; Claret, F. X.; Rassidakis, G. Z. Activation of mammalian target of rapamycin signaling pathway contributes to tumor cell survival in anaplastic lymphoma kinase—positive anaplastic large cell lymphoma. *Cancer Res.* **2006**, *66*, 6589−6597.

(47) Kumar, P.; Benedict, R.; Urzua, F.; Fischbach, C.; Mooney, D.; Polverini, P. Combination treatment significantly enhances the efficacy of antitumor therapy by preferentially targeting angiogenesis. *Lab Invest.* **2005**, *85*, 756−767.

(48) Wagner, E. F.; Nebreda, A. R. Signal integration by JNK and p38 MAPK pathways in cancer development. *Nat. Rev. Cancer* **2009**, *9*, 537−549.

(49) Bradham, C.; McClay, D. R. p38 MAPK in development and cancer. *Cell Cycle* **2006**, *5*, 824−828.

(50) Manke, I. A.; Nguyen, A.; Lim, D.; Stewart, M. Q.; Elia, A .E.; Yaffe, M. B. MAPKA P kinase-2 is a cell cycle checkpoint kinase that regulates the G2/M transition and S phase progression in response to UV irradiation. *Mol. Cell* **2005**, *17*, 37−48.